# Charge localization by static and dynamic distortions of the $MnO_6$ octahedra in perovskite manganites

P. G. Radaelli
*Institut Max Von Laue-Paul Langevin, Boîte Postale 156, 38042 Grenoble Cedex 09, France*

M. Marezio
*MASPEC, Consiglio Nazionale delle Ricerche, via Chiavari 18A, 43100 Parma, Italy*

H. Y. Hwang
*AT&T Bell Laboratories, Murray Hill, New Jersey 07974*
*and Joseph Henry Laboratory of Physics, Princeton University, Princeton, New Jersey 08544*

S-W. Cheong and B. Batlogg
*AT&T Bell Laboratories, Murray Hill, New Jersey 07974*
(Received 6 June 1996)

We present transport and neutron-diffraction data establishing a clear link between static and dynamic distortions of the $MnO_6$ octahedra and charge mobility in $A_{1-x}A'_x$ $MnO_3$ ($A$=La or Pr; $A'$=Ca or Sr). Systematic analysis of the Mn-O bond lengths versus average $A$-site ionic radius indicates that increasing static coherent $MnO_6$ distortion is associated with increasing insulating behavior and decreasing $T_C$. Furthermore, we observed a sudden drop of the oxygen thermal parameters at $T_C$, indicating that static incoherent and dynamic effects are also important. [S0163-1829(96)07538-8]

Manganese perovskites with general formula $A_{1-x}A'_x$ $MnO_3$ ($A$=La, Pr, Y, . . . ; $A'$=Ca, Sr, Ba, . . . ) have been the subject of renewed interest, due to the magnetoresistance (MR) exhibited near the ferromagnetic (FM) spin ordering temperature $T_C$. For the electronic hole doping concentration of $x\sim 0.30$, the high-temperature paramagnetic state is a poor electrical conductor, whereas the low-temperature FM state is metallic. Shortly after the discovery of these compounds some forty years ago,[1] the concept of double exchange has been developed to describe the essential aspects of the magnetic interactions between the Mn ions, which, due to the divalent substitutions for La on the $A$ site, are in a mixed-valence state $(+3/+4)$.[2–4] At present, there is strong disagreement on whether theoretical models based on double exchange alone can account quantitatively for the observed transport and magnetic properties of manganites.[5,6] Although first introduced by Goodenough,[7] upon the more recent renaissance of manganite research an additional important aspect has been reintroduced in the discussion of the physics of manganites: lattice distortions due to the different ionic size of $Mn^{+3}$ and $Mn^{+4}$ in general, and Jahn-Teller (JT)-type distortions of the oxygen octahedra around $Mn^{+3}$ in particular.[6,8] For instance, the crystal structure of the parent compound $LaMnO_3$ (Refs. 9 and 10) can be interpreted in terms of a static coherent JT distortion. However, for the manganites with optimized magnetoresistance, e.g., $La_{0.7}Sr_{0.3}MnO_3$, the space group (trigonal $R3c$) enforces on average equal Mn-O bond lengths, and thus prevents static coherent JT-type distortions of the $MnO_6$ octahedra. For the trigonal compounds, Millis and co-workers proposed a dynamic model,[6,8] in which temporally (and spatially) fluctuating local JT distortions would localize the conduction-band electrons as polarons above $T_C$. Such an effect would manifest itself in a diffraction experiment as a sudden drop of the Debye-Waller factors of the oxygen atoms below $T_C$. However, recent neutron-diffraction experiments have indicated that no obvious JT-type distortions exist in trigonal $La_{0.7}Sr_{0.3}MnO_3$.[11] MR is also observed in compounds, such as $La_{0.7}Ca_{0.3}MnO_3$, forming in orthorhombic $Pnma$ structure. In fact, MR tends to be large in orthorhombic phases with relatively low $T_C$. The $Pnma$ space group allows three independent Mn-O bonds, and can therefore accommodate a static coherent distortion of the $MnO_6$ octahedra. Alternatively, the insulating behavior could be associated with the formation of ''charge-ordering'' (CO) polarons, in which the lattice would distort around localized holes, due to the smaller radius of $Mn^{4+}$ with respect to $Mn^{3+}$. This view is supported by the observation, in $Pr_{0.7}Ca_{0.3}MnO_3$ and $La_{0.5}Ca_{0.5}MnO_3$, of a charge-ordered antiferromagnetic insulating phase at low temperature, which is competitive with the FM metallic phase.[12] Since CO distortions cannot be accommodated either in the $R3c$ or in the $Pnma$ space groups, they must necessarily be incoherent, in the absence of a symmetry change. However, both JT and CO distortions, either static or dynamic are expected to be primarily of the *metric* type, i.e., associated with a splitting of the Mn-O bond *lengths*, as opposed to a distortion of the bond *angles*.

Here, we present transport and diffraction data evidencing static and dynamic $MnO_6$ distortions associated with the metal-insulator transition for orthorhombic $A_{1-x}A'_xMnO_3$ samples ($x$=0.25, 0.30). High-temperature transport measurements show a sudden drop in resistivity with increasing temperature at the $Pnma\rightarrow R3c$ transition, indicating the

 

presence in the orthorhombic phase of an additional charge carrier localization mechanism that is absent in the trigonal phase. Neutron-powder-diffraction data obtained on a series of orthorhombic $A_{0.7}A'_{0.3}MnO_3$ samples with variable $A$-site ionic radius $\langle r_A \rangle$ show that increasing insulating behavior and decreasing $T_C$ with reduced $\langle r_A \rangle$ is directly associated with increasing static coherent $MnO_6$ distortion. Temperature-dependent neutron-powder-diffraction data, obtained on $La_{0.75}Ca_{0.25}MnO_3$, show a sudden decrease of static coherent $MnO_6$ distortions at $T_C$ with decreasing temperature. This effect is associated with a sharp volume anomaly. Furthermore, for $La_{0.75}Ca_{0.25}MnO_3$, the anisotropic Debye-Waller factors *parallel* to the Mn-O bond lengths have a discontinuity at $T_C$. This observation suggests that dynamic (or static incoherent) $MnO_6$ distortion effects of the *metric* type, as well as static coherent effects, are present in the orthorhombic phase. These results provide a strong support for theoretical models in which static and dynamic metric distortions of the $MnO_6$ octahedra play a significant role in determining the unusual transport properties of perovskite manganites.

Polycrystalline samples of $A_{1-x}A'_xMnO_3$ ($A$=La, Pr; $A'$=Ca, Sr, Ba) were synthesized through conventional solid state reaction in air. Electrical resistivity $\rho$ was measured using the standard four-probe technique. Neutron-powder-diffraction data were collected with the D2B diffractometer of the Institute Laue-Langevin at various temperatures between 2 and 300 K in the high-intensity mode, using a wavelength of 1.594 Å. Structural parameters were refined by the Rietveld method, using the program GSAS. For each composition, $\langle r_A \rangle$ was calculated using the tabulated values of Ref. 13. For ferromagnetic samples, a simple model with collinear Mn moments, to be refined, was sufficient to describe the magnetic scattering at the present instrumental resolution. One sample of the series, with composition $Pr_{0.7}Ca_{0.3}MnO_3$, displayed a very complex magnetic structure, with the coexistence of both ferromagnetism and antiferromagnetism. The antiferromagnetic component of this structure contains two propagation vectors ($\frac{1}{2}00$ and $\frac{1}{2}0\frac{1}{2}$), associated with two Mn sublattices.[14]

Figure 1 shows the behavior of $d\log\rho/dT$ as a function of temperature for four samples of composition $La_{0.70}Ca_{0.30-x}Sr_xMnO_3$ ($x$=0, 0.05, 0.09, and 0.13). As an example, the original $\log(\rho)$ vs $T$ curve for $x$=0 is shown in the inset. The sharp peaks below ~400 K are the signatures of the metal-insulator transition, which occurs at $T_C$. While increasing $\langle r_A \rangle$ from 1.205 Å for $La_{0.70}Ca_{0.30}MnO_3$ to 1.222 Å for $La_{0.70}Ca_{0.17}Sr_{0.13}MnO_3$, $T_C$ increases from 244 to 309 K.[15] At higher temperatures, a smaller negative peak is present in all the curves, indicating a sudden drop in $\rho$ upon heating. Diffraction measurements have shown that this feature is associated with the crossing of the $Pnma \rightarrow R\bar{3}c$ structural phase transition temperature $T_S$.[16] The results in Fig. 1 demonstrate that reducing $T_C$ with decreasing $\langle r_A \rangle$ correlates with increasing $T_S$ (see phase diagram in Fig. 2). It is noteworthy that, of the two phases at the transition, the $R\bar{3}c$ phase shows the lowest $\rho$. This observation can be understood by considering that, in the orthorhombic phase, additional charge localization is provided by a static coherent distortion of the $MnO_6$ octahedra, involving a splitting of the

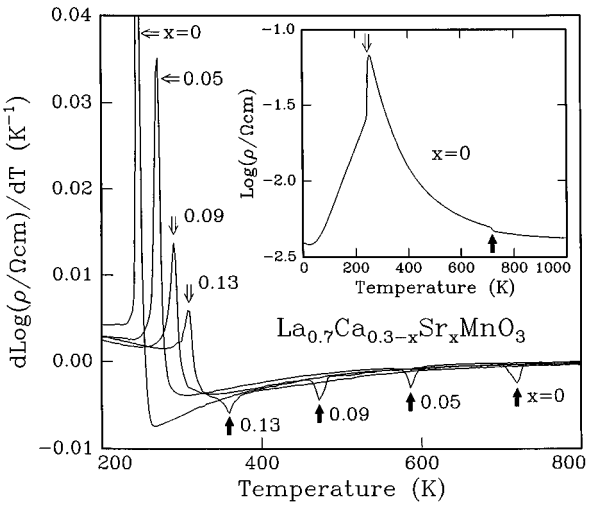


FIG. 1. Link between the $Pnma \rightarrow R\bar{3}c$ structural transition and resistivity. $d\log_{10}\rho/dT$ as a function of temperature for $La_{0.7}Ca_{0.3-x}Sr_xMnO_3$ ($x$=0, 0.05, 0.09, and 0.13). Filled and open arrows indicate the orthorhombic-trigonal phase transition temperature $T_S$ and the Curie temperature $T_C$, respectively. Inset: $\log(\rho)$ vs temperature for $La_{0.7}Ca_{0.3}MnO_3$.

Mn-O bond lengths. Such distortion must necessarily disappear at $T_S$, since all three Mn-O distances become equal by symmetry in the $R\bar{3}c$ phase. Here, a *static coherent* distortion of the $MnO_6$ octahedra has the meaning of a frozen-in breathing mode that is *coherent* over a scale of the order of or larger than the coherent length of the diffraction probe (~2000 Å). In a diffraction experiment, this type of distortion is associated with macroscopic strain, additional Bragg reflections, and lowering of the space group symmetry, which allows the three Mn-O bond lengths to be crystallographically independent. Conversely, an *incoherent* distortion is subject to temporal *(dynamic)* and/or short-range spatial *(static disordered)* fluctuations. In this case, the space group symmetry would allow only a *single* Mn-O distance

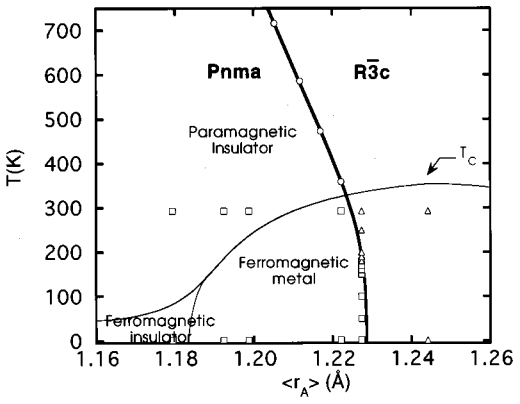


FIG. 2. High-temperature structural phase diagram of the $A_{0.7}A'_{0.3}MnO_3$ system ($A$=La, Pr; $A'$=Ca, Sr, Ba) as a function of $\langle r_A \rangle$. The two crystallographic phase regions are presented with different shadings and separated by a thick line. The $T_C$ and metal-insulator transition curves (from Ref. 15) are shown as thin lines. Neutron-diffraction data sets are shown as squares ($Pnma$) and triangles ($R\bar{3}c$). Open circles are from high-temperature resistivity.

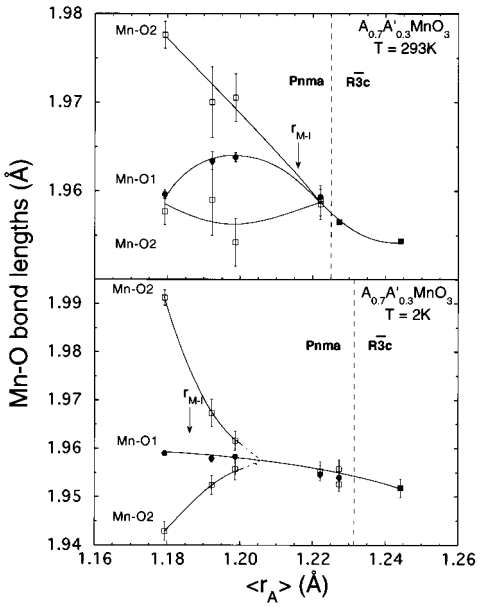


FIG. 3. Static coherent distortion of the $MnO_6$ octahedra as a function of $\langle r_A \rangle$ for $A_{0.7}A'_{0.3}MnO_3$. Mn-O bond lengths at 2 K (lower) and 293 K (upper). The dashed lines separate the different structural phases. Error bars are either shown or smaller than the symbols. Solid lines are guides to the eyes.

(the symmetry-breaking reflections would be broadened into the diffuse background). However, the incoherent atomic displacements with respect to the lattice-averaged positions will reduce the scattered intensities at large momentum transfers, and would, therefore, mimic large Debye-Waller factors. As already pointed out, the $R\bar{3}c$ symmetry would not be incompatible with an incoherent distortion.

Further evidence for the importance of static coherent $MnO_6$ distortions in the *Pnma* phase is provided by the behavior of the three Mn-O bond lengths as a function of $\langle r_A \rangle$, shown in Fig. 3 at 293 K (top) and 2 K (bottom). As a function of $\langle r_A \rangle$, the insulator-metal transition occurs, for each temperature, at a specific value $r_{M\text{-}I}$ with $r_{M\text{-}I}=1.185$ and 1.216 Å at 2 and 293 K, respectively. The figure shows that a static coherent distortion of the $MnO_6$ octahedra is present below $r_{M\text{-}I}$. With increasing $\langle r_A \rangle$, this distortion decreases and finally disappears above $r_{M\text{-}I}$. It should be noted that, for the orthorhombic samples with $\langle r_A \rangle$ much greater that $r_{M\text{-}I}$, all three Mn-O bond lengths are *equal* within the experimental uncertainty, although no symmetry constraint imposes such inequality. At room temperature, the $MnO_6$ distortion appears to be of the ''tetragonal'' type (normally associated with the ideal JT splitting), one Mn-O bond length being much larger than the other two. At 2 K, the two Mn-O2 bond lengths are split more symmetrically around the Mn-O1 (''orthorhombic'' distortion), but this does not rule out the JT mechanism, as the distortion in $LaMnO_3$, which is thought to be a classic JT example, is markedly orthorhombic.[9,10] Once again, our observations can be explained with the removal in the metallic phase of the static coherent distortion of the $MnO_6$ octahedra as one of the charge localization mechanism. It should be pointed out that, at least at low temperatures, there is still a measurable value of the distortion at $r_{M\text{-}I}$. A possible explanation is the existence of an upper critical value of the static distortion for metallization.

A stringent test of the relevance of octahedral distortion for charge localization is provided by the temperature dependence of the structural parameters. If static and/or dynamic distortions do localize charge carriers above $T_C$, then they must necessarily decrease or disappear at and below $T_C$. A recent synchrotron radiation work showed that, for orthorhombic $La_{0.75}Ca_{0.25}MnO_3$, the lattice parameters and the cell volume have a sharp anomaly at $T_C$,[17] implying a rearrangement of the internal structural parameters. In this study, we present the temperature variation of these parameters for $La_{0.75}Ca_{0.25}MnO_3$ as determined by neutron powder diffraction. We remark that similar effects were measured for several orthorhombic samples with different values of both $x$ and $\langle r_A \rangle$, suggesting that they are a universal property of the orthorhombic phase. The Mn-O bond lengths and the projections of the oxygen anisotropic Debye-Waller ellipsoids

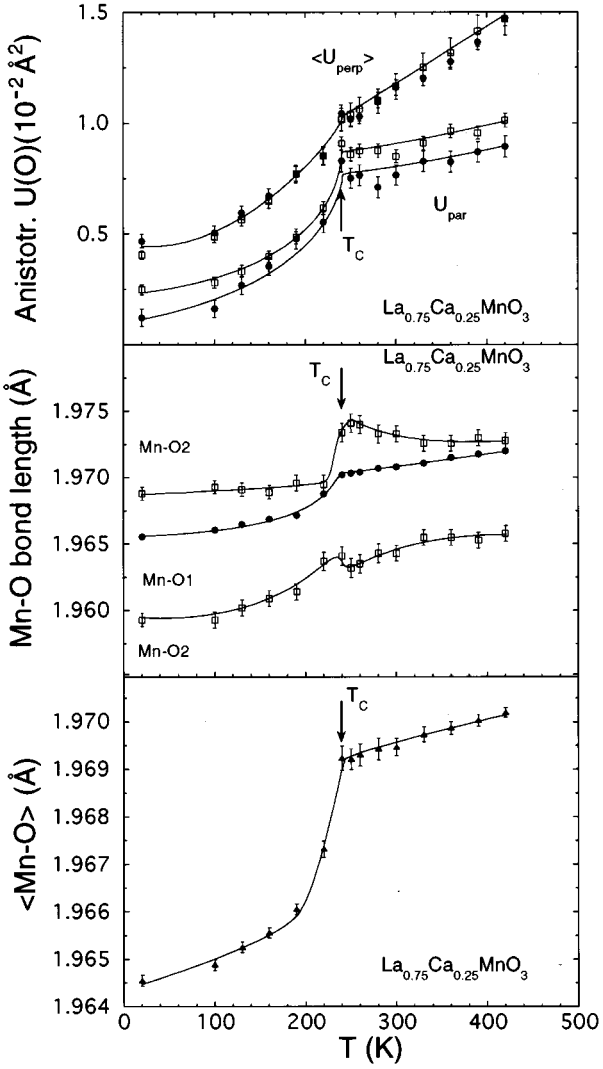


FIG. 4. Coherent and incoherent distortions of the $MnO_6$ octahedra vs temperature, for $La_{0.75}Ca_{0.25}MnO_3$. Average Mn-O bond length (lower), individual Mn-O bond lengths (center) and projections of the oxygen anisotropic Debye-Waller factors *parallel* ($U_{\text{par}}$) and *perpendicular* ($\langle U_{\text{perp}} \rangle$) to the direction of the Mn-O bond lengths for O1 (filled circles) and O2 (open squares) (upper).

$U_{ij}$(O1) and $U_{ij}$(O2) ($U=\langle u^2\rangle$) *parallel* and *perpendicular* to the direction of the Mn-O bonds ([010] and [101] for O1 and O2, respectively), as a function of temperature, as obtained by Rietveld refinements of neutron-powder-diffraction data, are shown in Fig. 4 (center and top panels, respectively). Above $T_C$, $U_{\rm par}$(O1) and $U_{\rm par}$(O2) are quite large and weakly temperature dependent. This is a clear signature of the presence of a disordered displacement field (spatial and/or temporal). At $T_C$, $U_{\rm par}$(O1) and $U_{\rm par}$(O2) suddenly drop and acquire a pronounced temperature dependence, indicating a crossover into a typical phonon regime. On the contrary, the average perpendicular components $\langle U_{\rm perp}\rangle$(O1) and $\langle U_{\rm perp}\rangle$(O2) display a much smaller anomaly, indicating that the incoherent effect is primarily of the *metric* type.

Further evidence is gained by analyzing the temperature dependence of the three Mn-O bond lengths. In the temperature range 500–240 K, the $MnO_6$ octahedral distortion tends to *increase* with decreasing temperature. However, the difference among the three Mn-O bond lengths is drastically and abruptly reduced at $T_C$, mainly due to a *decrease* of the largest of the Mn-O2 bond lengths. The short Mn-O2 bond and the Mn-O1 bond also show smaller but significant anomalies. The difference in the absolute value of the Mn-O2 discontinuities produces a decrease of the average Mn-O bond length $\langle$Mn-O$\rangle$ (Fig. 4, bottom panel) and, as a consequence, of the volume of the $MnO_6$ octahedra. The $\langle$Mn-O$\rangle$ contraction originates from the formation of metallic bonding in the ferromagnetic phase. In the light of these results, we conclude that, in the orthorhombic phase, the metal-insulator transition is associated with a sudden and significant decrease of both static coherent and dynamic (or static incoherent) distortions of the $MnO_6$ octahedra. These results lend a strong support to those theoretical models which include the effect of these distortions in their calculations. To the extent that these structural effects can be interpreted as arising from JT-type distortions, they are in qualitative agreement with the theoretical predictions by Millis *et al.*[8] However, the strong incoherent effects could also be interpreted in terms of the formation of CO ''$Mn^{+4}$'' polarons, the coherent JT-type component being a secondary effect induced in the now predominantly $Mn^{+3}$ matrix. These two scenarios cannot be distinguished from the present data.

In this study we have established experimentally a clear link between static and dynamic distortions of the $MnO_6$ octahedra and charge mobility. A sudden drop in $\rho$ at $T_S$ can be explained by a loss of static coherent distortion of the $MnO_6$ octahedra in the trigonal phase. In the orthorhombic phase, static distortion of the octahedra is always large in the insulating state, and always small or absent in the metallic state. As a function of temperature, a drop of the oxygen Debye-Waller factors as well as of the static distortion of the $MnO_6$ octahedra indicate that both static coherent and dynamic (static incoherent) effects are important ingredients for a complete picture of the magnetic and electric properties of perovskite manganites.


[1] G. H. Jonker and J. H. V. Santen, Physica **16**, 337 (1950).
[2] C. Zener, Phys. Rev. **82**, 403 (1951).
[3] P. W. Anderson and H. Hasegawa, Phys. Rev. **100**, 675 (1955).
[4] P.-G. de Gennes, Phys. Rev. **118**, 141 (1960).
[5] N. Furukawa, J. Phys. Soc. Jpn. **64**, 2734 (1995).
[6] A. J. Millis, P. B. Littlewood, and B. I. Shraiman, Phys. Rev. Lett. **74**, 5144 (1995).
[7] J. B. Goodenough, Phys. Rev. **100**, 564 (1955).
[8] A. J. Millis, B. I. Shraiman, and R. Mueller, Phys. Rev. Lett. **77**, 175 (1996).
[9] M. A. Gilleo, Acta Crystallogr. **10**, 161 (1957).
[10] P. Norby, I. G. K. Andersen, E. K. Andersen, and N. H. Andersen, J. Solid State Chem. **119**, 191 (1995).
[11] M. C. Martin, G. Shirane, Y. Endof, K. Hirota, Y. Morimoto, and Y. Tokura (unpublished). During the elaboration of this paper, we became aware of recent neutron-powder-diffraction results obtained by P. Dai *et al.* and by D. N. Argyriou *et al.*, evidencing the presence of distortions of the $MnO_6$ octahedra in $La_{0.65}Ca_{0.35}MnO_3$ and $La_{0.875}Sr_{0.125}MnO_{3+\delta}$, respectively.
[12] H. Yoshizawa, H. Kawano, Y. Tomioka, and Y. Tokura, Phys. Rev. B **52**, R13 145 (1995).
[13] R. D. Shannon, Acta Crystallogr. A **32**, 751 (1976).
[14] Z. Jirák, S. Krupicka, Z. Simsa, M. Dlouhá, and S. Vratislav, J. Magn. Magn. Mater. **53**, 153 (1985).
[15] H. Y. Hwang, S.-W. Cheong, P. G. Radaelli, M. Marezio, and B. Batlogg, Phys. Rev. Lett. **75**, 914 (1995).
[16] A. Asamitsu, Y. Morimoto, Y. Tomioka, T. Arima, and Y. Tokura, Nature (London) **373**, 407 (1995).
[17] P. G. Radaelli, D. E. Cox, M. Marezio, S.-W. Cheong, P. E. Schiffer, and A. P. Ramirez, Phys. Rev. Lett. **75**, 4488 (1995).